Dynamic RIS-Enabled Massive MIMO NOMA Systems Power Allocation Optimization for 6G Using Machin learning Approach/ Original article

Mohamed Hassan[1], Khalid Hamid[2], Salah Hagahmoodi[3], Elmuntaser Hassan[4],

1,2 Department of Electrical Engineering, Omdurman Islamic University, Omdurman, Sudan

1 mhbe4321@gmail.com, 2 khalid.bilal@oiu.edu.sd

3 Salah Hagahmoodi, Department of Information Technology, College of Computer Science and Information Technology, Almoughtarbeen University, Sudan.

salahhagahmoodi@gmail.com mailto:salahhagahmoodi@gmail.com

4 Department of Computer Science, Al-Neelain University, Khartoum, Sudan

3 Habba86@hotmail.com

Corresponding Author: Salah Hagahmoodi, salahhagahmoodi@gmail.com

Abstract

This study examines spectral efficiency (SE) and throughput throughout a spectrum of user densities (from 50 to 1000 users), user mobility speeds (0 to 350 km/h), latency, packet loss, and fairness index, within a wide range of signal-to-noise ratios (SNRs). The analysis includes a number of different situations, such as (i) cooperative non-orthogonal multiple access (NOMA) with massive multiple-input multiple-output (mMIMO), (ii) mMIMO cooperative NOMA integrated with cognitive radio (CR), and (iii) CR-assisted mMIMO cooperative NOMA enhanced with reconfigurable intelligent surfaces (RIS). All of these are part of 6G millimeter-wave (mmWave) networks. The study investigates the enhancement of latency, packet loss, and fairness index in proposed systems by a unique approach that dynamically optimizes power distribution via a Q-learning algorithm. The mathematical clarification of each equation provides a comprehensive understanding of signal reception by users, the dynamics and implications of CR, and the influence of intelligent RIS optimization on it. The results show that adding the IRS improves resource allocation, makes users perform better in crowded areas, lowers latency and packet loss, and raises the fairness index by reducing interference and making channel access more efficient, especially when using the suggested optimization algorithm. The results help 6G technology move further with scalable and efficient communication networks.

Keywords: cooperative NOMA, Massive MIMO, CR, reconfigurable intelligent surfaces (RIS), SE, millimeter wave (mmWave).

1. Introduction

Every generation of wireless networks, from first-generation (1G) to sixth-generation (6G), has seen enhancements in capacity and quality of service [1-3]. Establishing a 6G network necessitates surmounting several technological challenges, such as the implementation of intricate coding methodologies, enhanced frequency bands, and the development of novel antenna technologies. The 6G wireless network aims to achieve several goals, including reduced latency, increased throughput, extensive connection, and enhanced energy and spectrum economy. The volume of data transmission has increased markedly recently due to the widespread use of intelligent devices and equipment. Significant advancements have been made in the terahertz (THz) and millimeter-wave (mmWave) domains to meet the anticipated high demand [4-6]. To commence the 6G network, it is important to tackle technological problems such as the improvement of coding procedures, the optimization of frequency bands, and the advancement of antenna technology. 6G technology is expected to transform several industries upon its implementation due to its ability to provide enhanced degrees of immersion and engagement. The included industries include healthcare, transportation, and entertainment. Future communication networks are expected to demonstrate a substantial demand for 6G wireless technology. Wireless devices and services, including VR/AR, the Internet of Everything, and virtual reality, are seeing increased popularity and widespread acceptance, hence presenting new obstacles to create wireless networks of the future. The demand for varied data transfer, increased connection density, reduced latency, and optimal bandwidth utilization intensifies these challenges.

Various multiple-access algorithms exist, including non-orthogonal multiple access (NOMA). As seen in [7-8], NOMA can increase spectral efficiency (SE) and user throughput service. Receivers in mobile devices reduce beam-induced interference by the application of successive interference cancellation (SIC) techniques. According to [9], the fundamental concept of NOMA allows for the integration of many users by categorizing them based on cost or time. The greater the number of individuals utilizing NOMA, the more orthogonal resources become available [10-11]. The advancement of NOMA is anticipated to address these difficulties. These systems efficiently accommodate a substantial number of users owing to their optimized architecture and reduced resource consumption [12]. A compelling option that demonstrates the potential for enhancing data throughput in mmWave and THz communication systems is massive multiple-input multiple-output (mMIMO) NOMA [13-14].

Cognitive radio (CR) technology is an effective method for spectrum management, providing opportunistic, on-demand connections that resolve capacity challenges in traditional licensed wireless communication networks. Primarily, in CR-based networks, there are PUs, or authorized users, and SUs, or unauthorized users. The SUs aims to exploit any opportunities that arise while they contend with the PUs for licensed spectrum [15-16]. Consequently, CR technology will be essential in the advancement of future wireless networks and in meeting their exceedingly quick demands [17].

An approach to creating intelligent and efficient radio configurations is the idea of reconfigurable intelligent surfaces (RIS) [18- 19-20]. A compilation of passive reflecting elements (RE) forms RIS, which systematically alter the phase and amplitude of incoming signals. However, comprehensive spatial

communication is unattainable with traditional RIS systems that rely solely on reflection. A proposed solution to this issue, as shown in [21], is STAR-RIS, which denotes simultaneous transmission and reflection employing RIS.

Recent research on mMIMO-NOMA in mmWave/THz networks has predominantly overlooked user clustering in favor of performance analysis. To meet the increased expectations for spectral efficiency and multiple user connections in 6G, NOMA-enabled networks must also include organizational user grouping. Moreover, user clustering in networks functioning in low-frequency bands has garnered considerable study attention, but mmWave/THz networks remain largely unexamined. Nonetheless, investigations on user pairing in the context of clustering users within a MIMO-NOMA system are limited to a restricted number of users [22-23]. Recent studies classify users as cellular or device-to-device (D2D) via a cluster-matching technique grounded in channel correlation [24].

This method converts user clustering into a polynomial problem. Despite its general simplicity, a hurdle in learning-assisted clustering systems is the insufficient initialization of cluster heads. The efficacy of the STAR-RIS-based system for simultaneous transmission and reflection in fading channels has been previously examined by a compendium of authors [25-26]. The findings indicate that STAR-RIS surpasses conventional RIS in NOMA systems, especially for users located at the cell periphery lacking a direct line of sight (LoS) to the base station (BS). The authors illustrated that in low signal-to-noise ratio (SNR) scenarios, the inverse disproportionate allocation of resources in STAR-RIS can offset the BS's uneven power distribution, establishing that NOMA utilizing STAR-RIS remains effective despite the absence of a direct link between the BS and the users. In areas with a high

SNR, the impact of resource allocation is negligible. The authors performed a comprehensive examination of the efficacy of entire transmit power systems with STAR-RIS [27-28]. The evaluation of performance was conducted concerning both fault-free and non-fault-free cascade interference cancellation, as indicated in [29]. A comparison between NOMA and OMA communication systems was conducted in [30] within the context of phase-shifted coupled STAR-RIS.

The notion of RIS systems has become significant as an economical option for 6G wireless networks. Numerous cooperative NOMA configurations utilizing RIS have been mentioned in the literature. The downlink (DL) transmissions of a system model comprising one BS, two users, and one receiver-input-signal were analyzed in the work referenced as [31]. The concept of utilizing cooperative NOMA resulted in a reduction of the overall transmitted power. The study in [32] examined the application of RIS to enhance the efficiency of cell border users in a SWIPT NOMA system, where data is sent from a user at the cell core to a user at the cell boundary. In [33], researchers examined a two-stage RIS-assisted transmission approach for cooperative NOMA networks with SWIPT, which may enhance the attainable rate for strong users while maintaining the service quality requirements of weak users.

The future of wireless networks is characterized by CR NOMA. Multiple networks can share a single frequency due to CR's sophisticated monitoring and decision-making, enhancing spectrum utilization [34]. NOMA enhances connection, equity, and SE by allowing many users to share time, code, and frequency resources [35]. The ergodic capacity and outage probability (OP) were assessed from the fundamental critical route to evaluate the

performance of the NOMA-enhanced network [36]. To promote the use of NOMA systems among users with equivalent transmission power, the creators of [37] improved uplink communication by the incorporation of active and passive RIS. The objective of formulating a hybrid user clustering and RIS allocation approach was to improve the implementation of the NOMA scheme and optimize the system's aggregate rate [38]. The effectiveness of the RIS-enhanced NOMA network was analysed in [39], concentrating on energy efficiency in both delay-tolerant and delay-constrained modes. The authors of [40] developed a deep learning framework and assessed the RIS-assisted CR-NOMA system to forecast ergodic performance.

Currently, most research is on beamforming design employing RIS. Nevertheless, there are several peculiarities regarding our job. While no CR-NOMA network system model [41] presently exists, passive beamforming on RIS is the preferred approach after some simplifications. Therefore, the optimization procedures differ from our work. Thus, due to the characteristic optimization problem presented in [42], even when using analog conventions. The method examined in [43] differs significantly from ours in that we aim to optimize SE and throughput using the CR cooperative NOMA mMIMO network with DL assisted by intelligent RIS. The principal contributions encompass

This study introduces a unique mMIMO DL cooperative NOMA system for many users inside a 6G mmWave communication framework and utilizes clever intelligent RIS and CR. To demonstrate its scalability and adaptability in user-dense contexts, we evaluate it with different user counts (50 and 1000).

The impact of different mobility speeds on the effectiveness of CR mMIMO DL cooperative NOMA networks, ranging from 0 to 350 km/h, is analysed, considering scenarios with and without RIS. This element is crucial for understanding the robustness of intelligent RIS-assisted systems for high-mobility users.

The examination of user density and the impact of latency, packet loss, and SNR on fairness index throughput demonstrates the scalability of NOMA collaborative DL systems and suggests improvements to the network architecture.

This work employs a Q-learning algorithm to enhance power allocation, providing an adaptive method that enables the system to learn and modify power distribution according to network circumstances, hence optimizing latency, packet loss, and fairness index.

The succeeding portions of this work conform to this structure. Section II offers a detailed examination of the proposed models and approaches. Section III outlines the simulation parameters and reports the results. Section IV delineates the outcomes of these endeavours.

2. System Model

This study investigates wireless networks. The network comprises several mMIMO DL cooperative NOMA user groups that employ CR integration and mm-Wave technology as shown in Figure 1. Users are positioned at varying distances from the BS, leading to varied received power levels. The network utilizes 512-quadrature amplitude modulation (QAM). Number of users and the operating principles of cooperative NOMA inside the power domain (PD).

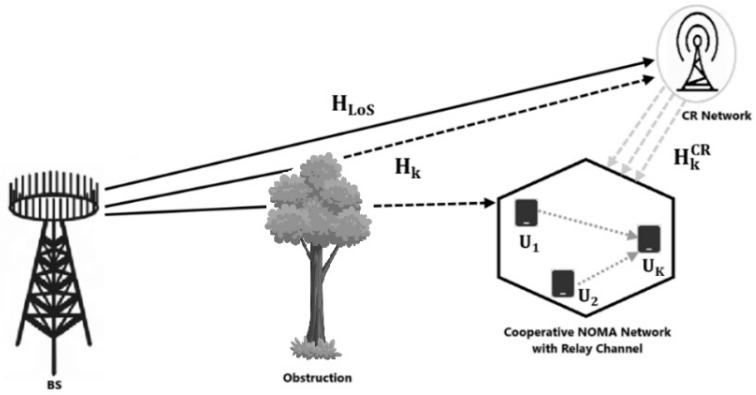

Fig.1 illustrates mMIMO PD DL mMIMO cooperative NOMA with k users employing CR and mmWave technology

In mMIMO, each BS possesses several antennas (M) and accommodates multiple users (N). The mMIMO will physically multiplex many users and focus energy in narrow beams on each user, enhancing data rates and spectrum efficiency. The mMIMO channel is represented for each user as a Rayleigh fading channel matrix. When there is no LoS path between the transmitter and receiver, Rayleigh fading happens. This makes the received signal made up of several separate, scattered parts. Modeling the BS (with M antennas) for user k channel, the $H_{\mathrm{k}} \in \mathbb{C}^{M\times 1}$ channel vector connecting the BS to the $k-th$ user [42].

$$H_{\mathrm{k}}=\left[h_{\mathrm{k,l}}, h_{\mathrm{k},2}, \ldots, h_{\mathrm{k},M}\right]^{T} \tag{1}$$

where is the system user index. $h_{\mathrm{k},M}$ is the channel coefficient between the kth user and the transmit antenna. M_T is the number of BS or transmitter transmitting antennas. The coefficient of the Rayleigh fading channel between the $m-th$ antenna at the BS and the $k-th$ user is denoted by the complex Gaussian random variable $h_{k,m} \sim C\mathcal{N}\left(0, \beta\mathrm{k}\right)$. User k perceives $\beta\mathrm{k}$ as large-scale route loss and shadowing. A formalizable univariate Gaussian

distribution is employed to determine the real and imaginary channel coefficients for Rayleigh fading.

$$y_{\mathrm{k}} = H_{\mathrm{k}}^{H} x + z_{\mathrm{k}} \tag{2}$$

where x is the BS broadcast signal, $z_{\mathrm{k}} \sim C\mathcal{N}\left(0, \sigma^2\right)$ is the AWGN with variance σ^2. CR comprises PUs, who are authorized to utilize certain frequency bands, and SUs, who can access unoccupied spectrum without disrupting the PUs. Spectrum sensing methodologies allow PUs to detect available channels. A power discovery technique is employed to assess channel occupancy by monitoring power levels, while the presence of primary users is identified using prior knowledge of their signal characteristics, mathematically described as follows.

$$E = \sum_{n=1}^{N} \left| \mathcal{Y}[n] \right|^2 \tag{3}$$

The receive signal $\mathcal{Y}[n]$, N samples. The spectrum sensing decision rule is [44],

$$\text{Decision} = \begin{cases} \mathrm{H}_0 & \text{if } E < \lambda \left(\text{spectrum available}\right) \\ \mathrm{H}_1 & \text{if } E \geq \lambda \left(\text{spectrum occupied}\right) \end{cases}$$

E is the signal energy and λ is the detection threshold. The available bandwidth, B_{avail}, is determined as follows,

$$B_{avail} = B_{total} - B_{occupied} \tag{4}$$

$B_{occupied}$ represents the bandwidth utilized by PUs ascertained using spectrum sensing. NOMA multiplexes PD users to share time-frequency resources. Channel conditions determine user power levels. The total power Pt is allocated among users based on their channel conditions.

$$P_k = P_t \cdot \frac{1}{k} \tag{5}$$

User index k (1st user has most power). In cooperative NOMA, user $k's$ received signal is,

$$y_k = H_k^H \sum_{\mathrm{n}=1}^{K} \sqrt{P_{\mathrm{k}}}\, x_{\mathrm{k}} + z_k \tag{6}$$

x_{k} is the transmitted signal, P_{k} is the power (higher for poorer channel conditions), and z_k is noise at user k. SIC lets better channel users decode and delete weaker channel users' signals before decoding their own. The SINR for k users as [11],

$$SINR_k = \frac{P_k \cdot h_k}{\sum_{j=1, j\neq k}^{K} P_j \cdot h_j + N_0} \tag{7}$$

For cooperative users, SINR additionally accounts for relayed signals [44],

$$SINR_{coop} = SINR_k + \sum_{j=1}^{k-1} SINR_j \tag{8}$$

Calculate the k^{th} user's SE_k,

$$SE_k = \frac{B}{K} \log_2 \left(1 + SINR_{coop}\right) \tag{9}$$

The diverse reflective elements of the intelligent RIS device can alter the phase of incoming electromagnetic waves, hence improving communication quality, as seen in Figure 2.

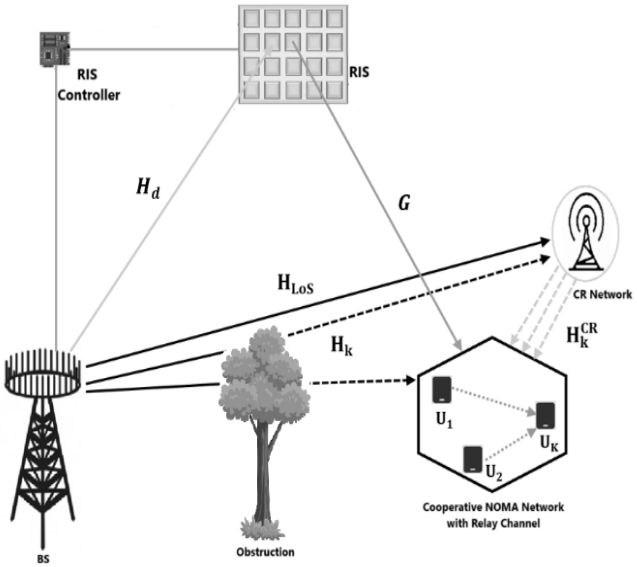

Fig. 2 illustrates mMIMO PD DL CR mMIMO cooperative NOMA with users employing intelligent IRS and mm-Wave methodologies

The RIS-assisted communication connection CSI channel model is,

$$H_{RIS} = G\Theta H_d \tag{10}$$

The BS-RIS channel is represented by $H_d \in \mathbb{C}^{N_{RIS} \times M}$, whereas the RIS-user channel is $G \in \mathbb{C}^{N \times N_{RIS}}$. The diagonal matrix $\Theta = diag(e^{j\theta_1}, e^{j\theta_2}, \ldots, e^{j\theta_{N_{RIS}}})$ represents the phase shifts caused by the RIS elements. The user received this RIS signal [42],

$$\mathcal{Y}_k^{RIS} = H_k^H x + g_k^H \Theta H_d x + z_k \tag{11}$$

where g_k is the RIS-user channel.

$$SINR_{RIS} = \frac{P_k \cdot |H_{RIS}|^2}{I + N_0} \tag{12}$$

where I is user interference. RIS signal intensity is greatly improved by optimizing phase shifts. Define optimization issue:

$$\max_{\theta} \left| H_{RIS} \right|^2 \tag{13}$$

Combining all components creates this cooperative NOMA system with RIS and CR for SE. Both direct and RIS-assisted user-BS connections employ the Rayleigh fading channel model. The user $k's$ effective NOMA system with RIS channel is,

$$h_{eff,\mathrm{k}} = H_{\mathrm{k}} + \mathrm{g}_{\mathrm{k}}^{H} \Theta H_{d} \tag{14}$$

The SE for user k in a NOMA system with RIS [46] is,

$$SE_{\mathrm{k}} = \log_2 \left(1 + \frac{P_{\mathrm{k}} \left| h_{eff,\mathrm{k}} \right|^2}{\sum_{i<\mathrm{k}} P_i \left| h_{eff,i} \right|^2 + \sigma^2} \right) \tag{15}$$

Calculate throughput T as,

$$T = SE_{total} \times B_{avail} \tag{16}$$

To calculate throughput with and without RIS, alter user density by changing the number of users k depending on area size A and density ρ, $K = \rho \times A$. Thus, user density affects throughput [47],

$$T_{with/without\ RIS}(\rho) = \sum_{k=1}^{\rho \times A} SE_{with/without\ RIS,k} \tag{17}$$

Changes in distance and relative velocities alter channel conditions when users move randomly. Let, $p_{\mathrm{k}}(t) = \left[x_{\mathrm{k}}(t), \mathcal{Y}_{\mathrm{k}}(t) \right]$ represent user $k's$ position at time t. v_{k} represents user iii's speed. θ_{k} represents user $k's$ random movement direction. The position of user k at time $t + \Delta t$ is,

$$p_{\mathrm{k}}(t+\Delta t)=p_{\mathrm{k}}(t)+v_{\mathrm{k}}\Delta t\cdot\left[cos(\theta_{\mathrm{k}}),sin(\theta_{\mathrm{k}})\right] \tag{18}$$

Mobility speed in m/s is represented by $vi \in MobilitySpeeds$. Modeling the BS-user channel uses path loss, small-scale fading, and user mobility. For user k at distance $d_{\mathrm{k}}(t)$, the path loss is [48],

$$PL_{\mathrm{k}}(t)=\left(\frac{4\pi d_{\mathrm{k}}(t)}{\lambda}\right)^{-\alpha} \tag{19}$$

All users' small-scale fading is modelled as Rayleigh fading channels. At time t , the BS-user k channel matrix $H_{\mathrm{k}}(t)$ is,

$$H_{\mathrm{k}}(t)=\sqrt{PL_{\mathrm{k}}(t)}\cdot\left(G_{\mathrm{k}}(t)+jB_{\mathrm{k}}(t)\right) \tag{22}$$

The real and imaginary channel sections are modelled by independent and identically distributed Gaussian random matrices $G_{\mathrm{k}}(t)$ and $B_{\mathrm{k}}(t)$. RIS channels connect users to the RIS. $H_{RIS,k}(t)$ represents the channel matrix for RIS-assisted user k at time t [49],

$$H_{RIS,k}(t)=\sqrt{PL_{RIS,k}(t)}\cdot\Phi(t)\cdot\left(G_{RIS,k}(t)+jB_{RIS,k}(t)\right) \tag{23}$$

The real and imaginary components of the channel from RIS to user k are $G_{RIS,k}(t)$ and $jB_{RIS,k}(t)$.

$$SINR_{RIS,k}(t)=\frac{P_k(t)\cdot\left|H_{RIS,k}(t)\right|^2}{\sum_{j<k}P_j(t)\cdot\left|H_{RIS,k}(t)\right|^2+N_0} \tag{25}$$

$$D=SE\times BW \tag{26}$$

where D is data rate (bps).

$$L=\frac{Data\ Size}{D}\times f(SNR) \tag{27}$$

Where L is latency, $f(SNR)$ is the channel-dependent factor for different channel models and user setups.

For each user, packet loss P_{loss} occurs if their SINR falls below a specified SINR threshold,

$$P_{loss} = \begin{cases} 1 & if\ SINR < SINR_{threshold} \\ 0 & otherwise \end{cases} \tag{28}$$

$$F = \frac{\left(\sum_{k=1}^{K} \Sigma r_k\right)^2}{K \cdot \sum_{k=1}^{K} r_k^2} \tag{30}$$

where F is fairness, r_k represents user $k's$ throughput, L_k represents user $k's$ latency, and β balances latency and fairness. The cooperative NOMA throughput, latency, and packet loss optimization approach is thoroughly analyzed, as seen in logarithm 1, focusing on the mathematical aspects of logarithmic power distribution and its effect on latency, packet loss and fairness index calculation. A broad goal is,

$$R = \sum_{k=1}^{K} r_k - \lambda \cdot L - \mu \cdot P \tag{31}$$

where R is System performance reward. r_k is user k throughput. K user total. L system aggregate latency. P System-wide packet loss. The weight factor λ balances throughput and latency. μ Weight factor for packet loss reduction. Each state *s* encapsulates pertinent attributes of the system:

$$s = \{SINR_1, SINR_2, \ldots, SINR_K,\ P_{alloc},\ PLR_1, PLR_2, \ldots, PLR_K\} \tag{32}$$

where power allocation P_{alloc}, user k (P_{Loss} R) packet loss ratio. Power allocation to each user is action as,

$$a = \{P_1, P_2, \ldots, P_K\} \tag{30}$$

a represents the power location of each user, determined by ȯ the probability of exploration.

$$R(s,a) = -\frac{1}{K}\sum_{k=1}^{K}\left(L_k + \mu \cdot P_{Loss} R_k\right) + \beta \cdot F \tag{31}$$

Based on the Bellman equation, Q-learning updates Q-values,

$$Q(s,a) \leftarrow Q(s,a) + \alpha\left[R(s,a) + \gamma a' max Q(s',a') - Q(s,a)\right] \tag{33}$$

Q-value for state s and action a; α = learning rate. Discount factor (γ factor). The maximum Q-value for the subsequent state s' over all potential actions s'. The procedure runs until Q values converge or for a set number of iterations. After that, the latency, packet loss and fairness are determined using equations (27, 29 and 30) respectively.

Algorithm 1. Q-Learning algorithm

1. Initialize the Q-Table and hyper parameters $(\alpha,\gamma,\varepsilon,\lambda,\mu,\beta)$
2. Commence ε:
   a) Initialize state s, encompassing $SINR, P_{alloc}, and\ P_{Loss}$ R for each user.
3. In the ε of convergence or maximum iterations:
   a) Select action according to the ε-greedy policy.
   b) Implement action (P_{K}) and monitor:
      - Subsequent state s'.
      - Reward $R(s,a)$ is determined by delay, packet loss, and fairness.
   c) Revise Q-value:
      $Q(s,a)\rightarrow Q(s,a)+\alpha * (R(s,a)+\gamma * max Q(s',a')-Q(s,a).$
   d) Update state $s\,to\,s'$.
4. End ε:
   a) Derive the best strategy for latency, packet loss, and equity.
5. Implement an effective power allocation strategy.
6. End.

3. Simulation Results and Discussion

The simulation parameters for the proposal systems model in 6G networks can be seen in Table 1. The results indicate the relationship between the scalability of these systems and the rise in user count, SNR, and throughput. The charts depict the results of many mMIMO cooperative NOMA scenarios, emphasizing the distinctions between configurations with

and without intelligent RIS and CR, with the impacts of mobility speed and network density on throughput and latency across different user densities.

Table .1 presents comprehensive details on the simulator settings employed for modeling proposal system networks

Parameter	Value
Number of Users	50 to1000
Mobility Speeds	0 to 350 Km/h
Number of Antennas	256x256
RIS Configuration	512x512
SNR (dB)	-20 to 40
Modulations	1024 QAM
Path-loss exp.	2.7
BW	30 G Hz
Cellular type	Microcells
Frequency Range	26 GHz to 40 GHz

Figure 3 shows the SE and SNR for 50 and 1000 users in the mmWave mMIMO DL CR cooperative NOMA PD system. The SE improved as the SNR rose. The group of 50 and 1000 users reaches a maximum SE of 2.0201 and 0.0952 bps/Hz, respectively, when the combination system is used with the intelligent RIS; the SE is enhanced by 72% and 58%, respectively, at the SNR of 40 dB.

The throughput and SNR for 50 and 1000 users in the mmWave mMIMO DL CR cooperative NOMA PD system are shown in Figure 4. The throughput improved as the SNR increased. The groups of 50 and 1000 users reach a maximum throughput of 12.2143 and 0.5692 Gbps, respectively, when the combination system is used with the intelligent RIS; the throughput is boosted by 76.2% and 98%, respectively, at the SNR of 40 dB.

The RIS system significantly improves the SE and throughput of the proposed system, especially as the number of users increases. This is

attributed to the fact that the RIS system improves signal quality by reducing interference and enhancing channel gain. This is evident in the large changes in the percentage of 1000 users. The results are better than [13-48-50].

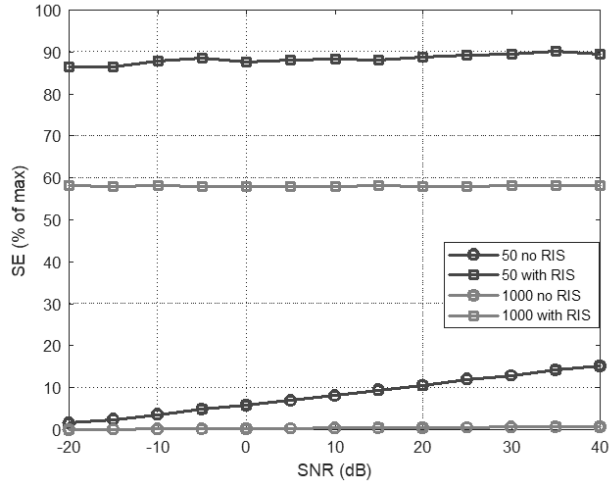

Fig. 3. SE versus SNR for 4 different groups of mMIMO DL CR cooperative NOMA users with and without intelligent RIS

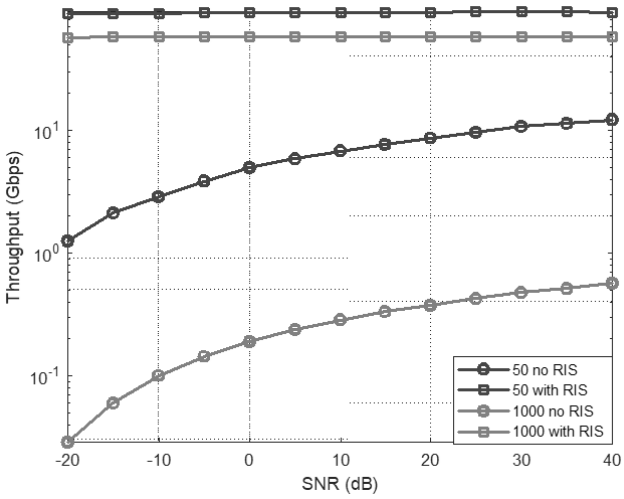

Fig. 4. Throughput vs. SNR for 4 different groups of mMIMO DL CR cooperative NOMA users with and without intelligent RIS

Figure 5a-b shows the throughput and mobility speed (from 0 to 350 km/h) for 100 users in the cooperative NOMA PD system with mmWave mMIMO DL CR technology, with and without the intelligent RIS. As speeds increased, the throughput decreased due to Rayleigh multipath vanishing.

Figure 5-a demonstrates that a system with a (-20 dB) SNR undergoes a more rapid decrease in throughput when mobility speed escalates, unlike the system using RIS. Mobility rates of 50 km/h intensify system attenuation, resulting in a significant reduction in throughput. The poor SNR causes the signal quality to deteriorate to such an extent that augmentation of transmission power is unable to maintain an acceptable throughput level; the results achieved surpass the findings of [49].

The system illustrated in Figure 5-b has the SNR of 40 dB. At low mobility rates (0 to 30 km/h), throughput is improved, especially with the application of RIS. The RIS enhances signal reception by efficiently reflecting or refracting signals in the desired direction. As mobility increases, the throughput decreases. RIS has no impact on enhanced throughput at high speeds (up to 350 km/h) compared with systems without RIS [51]; the obtained results are better. At a higher SNR level of 40 dBm, throughput always shows that greater transmission of power reduces losses caused by mobility.

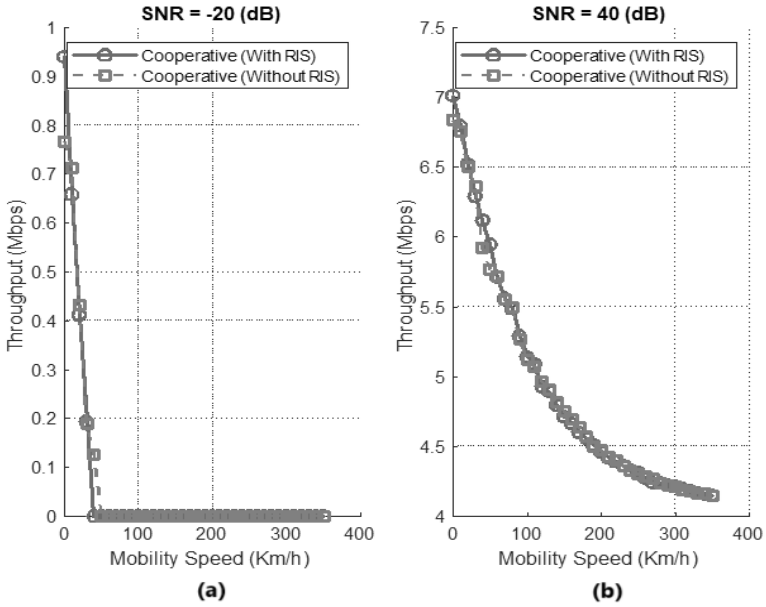

Fig. 5. Throughput against mobility speed for 100 mMIMO DL CR cooperative NOMA users with and without intelligent RIS

Figure 6 shows the mmWave mMIMO DL CR cooperative NOMA PD system with and without intelligent RIS. It shows the throughput and user density for different user numbers. Throughput reduces with the rising user density. The group of 1000 users achieved throughputs of 0.01 and 0.05 Gbps/Hz, as well as 0.21 and 1.1 Gbps/Hz, without and with intelligent RIS, at the SNR of -20 and 40 dB, respectively. A cohort of 50 users achieved throughputs of 0.1 and 0.33 Gbps/Hz, as well as 3.76 and 17.51 Gbps/Hz, without and with intelligent RIS, at SNR levels of -20 and 40 dB, respectively. The findings are better compared to those in [49].

As the user base expands, performance generally declines due to user interference and resource allocation. In cooperative NOMA systems, it is common for multiple users to compete for identical resources. RIS mitigates

the impact of user density by improving channel conditions and reducing interference, especially in high-user-density scenarios.

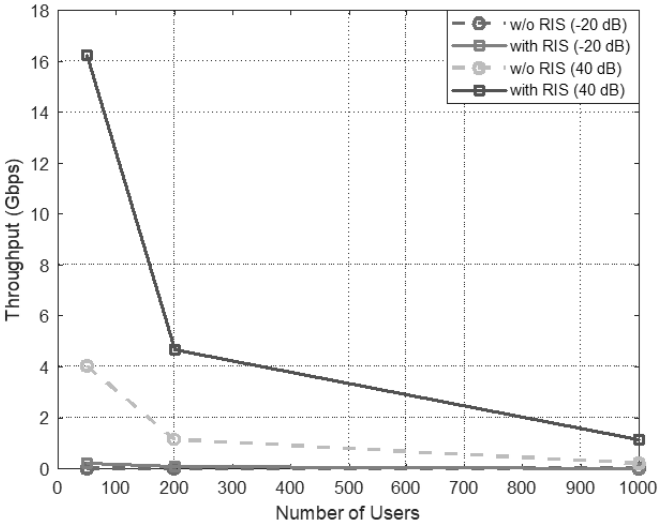

Fig. 6. Throughput versus user density of mMIMO DL CR cooperative NOMA users with and without intelligent RIS

Figure 7 illustrates how latency varies with the number of users in three systems: mMIMO cooperative NOMA, mMIMO CR cooperative NOMA, and mMIMO CR cooperative NOMA with intelligent RIS. As user competition for limited resources intensifies, network congestion and interference occur, leading to increased latency with more user density. mMIMO CR cooperative NOMA regularly exhibits higher latency than traditional NOMA utilizing the mMIMO method and mMIMO CR cooperative NOMA with RIS [52]. The heightened latency is due to the requirement to implement a coordination layer and perform channel sensing, which introduces further latencies from interference management and channel access.

The latency performance of mMIMO cooperative NOMA and mMIMO CR cooperative NOMA using intelligent RIS systems was 6.8% and 5% better at 50 users, respectively, than mMIMO CR cooperative NOMA, which had a latency of 0.31 ms. At a user density of 100, mMIMO cooperative NOMA and mMIMO CR cooperative NOMA using intelligent RIS systems had 9.5% and 6% better latency performance than mMIMO CR cooperative NOMA, which had a latency of 0.87 ms at the SNR of 40 dB; the outcomes surpass those of [44]. The mMIMO CR cooperative NOMA with an intelligent RIS system has superior latency performance, even at elevated user densities, positioning it as a formidable option for high-density 6G networks where interference control is essential.

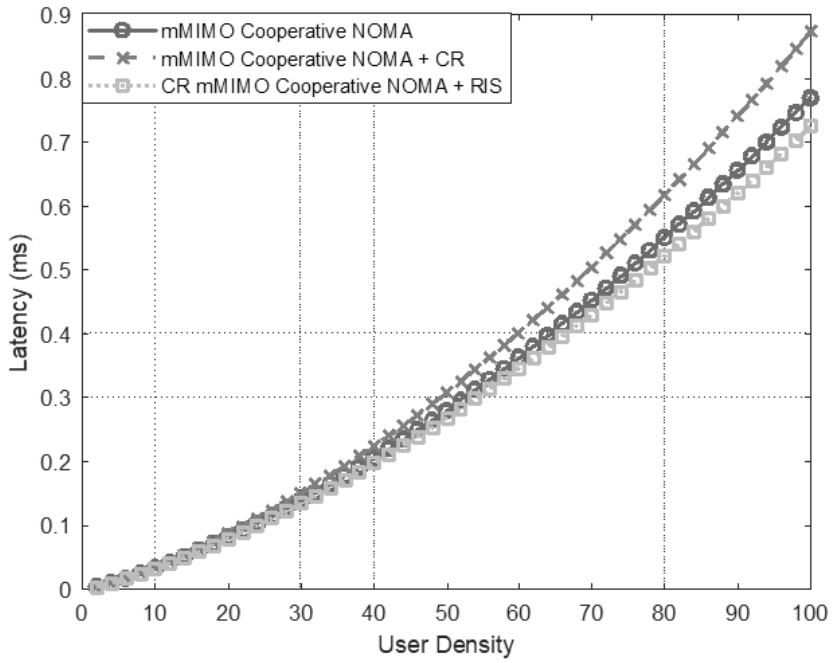

Fig. 7. Latency vs. user density for three various systems

Figure 8 exhibits the variation in latency relative to the number of users across three distinct systems: mMIMO cooperative NOMA, mMIMO CR cooperative NOMA, and mMIMO CR cooperative NOMA integrated with intelligent RIS utilizing a Q-learning algorithm. At a user density of 52, the latencies recorded are 0.21, 0.23, and 0.20 ms. With 100 users, the latencies for mMIMO cooperative NOMA, CR mMIMO cooperative NOMA, and CR mMIMO cooperative NOMA systems with the intelligent RIS of 40 dB SNR are 0.47, 0.51, and 0.45 ms, respectively. These results are better than those of [44-53]. Compared to the previous result, we find an improvement of 38.2%, 37.8%, and 38.4% for three scenarios due to a reduction in latency due to the use of the Q-learning algorithm for diverse power allocation strategies based on the variation of user density, which leads to greater stability in access time.

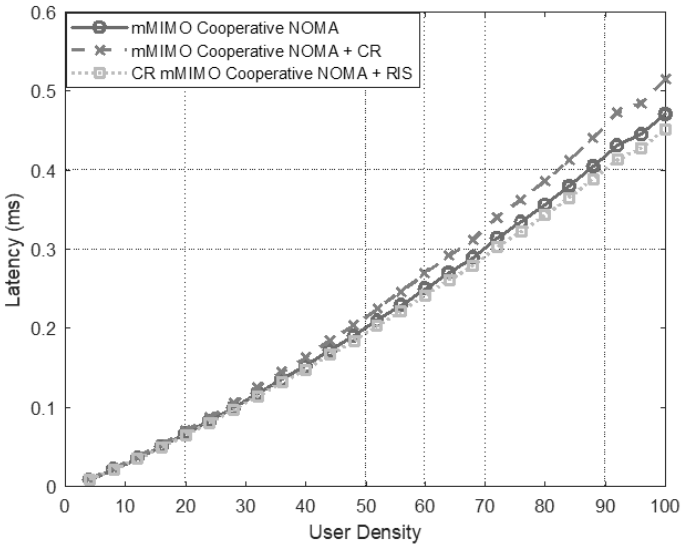

Fig. 8. Latency versus user density for three different scenarios with optimization algorithm

Figure 9 shows how packet loss varies with the number of users in three different systems: mMIMO cooperative NOMA, mMIMO CR cooperative NOMA, and mMIMO CR cooperative NOMA with intelligent RIS. At a user density of 50, the packet loss performance of three systems is 22%, 22.5%, and 21%, and at the user density of 100, the packet loss performance of three systems is 23.5%, 23.75%, and 22%, respectively, at the SNR of 40 dB. An increase in users results in greater interference and diminished resources, adversely affecting all systems. Optimal placement of RISs, phase adjustments, and additional strategies, such as user clustering and improved power distribution, can optimize performance.

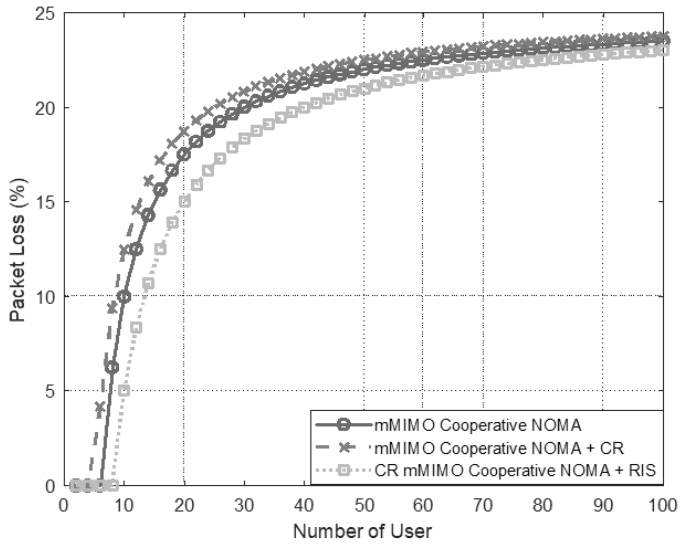

Fig. 9. Packet loss against user density for three different scenarios with optimization method

Figure 10 shows how packet loss changes with the number of users in three different systems: mMIMO cooperative NOMA, mMIMO CR cooperative

NOMA, and mMIMO CR cooperative NOMA with intelligent RIS integration with Q-learning logarithm. At a user density of 50, the packet loss performance of three systems is 9%, 12%, and 1%, and at the user density of 100, the packet loss performance of three systems is 17%, 18.5%, and 13%, respectively, at the SNR of 40 dB. The results show that utilizing Q-learning in conjunction with RIS greatly simplifies the problem of dealing with packet loss in dense cooperative NOMA systems. This method drastically reduces packet loss rates in situations with a high concentration of users. These results surpass those of [44-54].

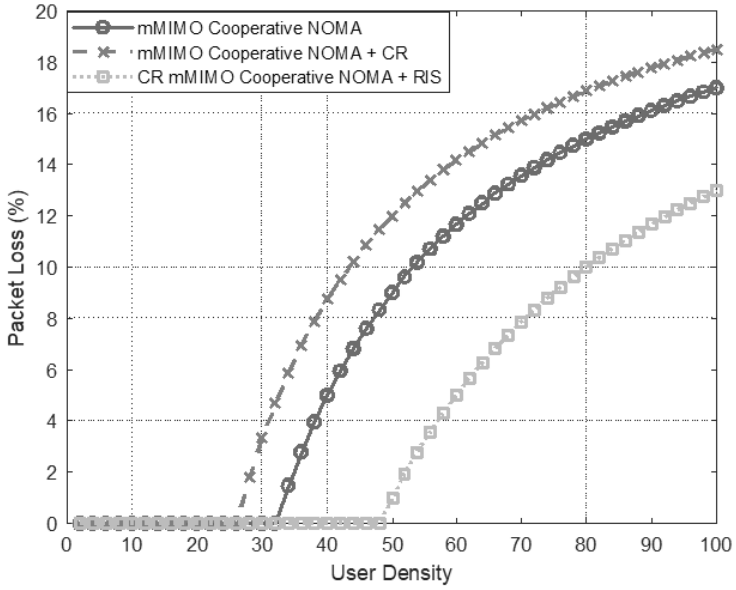

Fig. 10. Packet loss vs. user density for three different scenarios with Q-learning logarithm

Figure 11 displays the fluctuation in the fairness index in relation to SNR across three separate systems: the NOMA cooperative mMIMO system,

the NOMA cooperative mMIMO CR system, and the mMIMO cooperative NOMA CR system combined with intelligent RIS. The system is rather unstable in terms of fairness across different configurations and SNR levels, with fairness values that don't change much. CR and RIS seem to have little effect on justice, since they don't change much from the basic cooperative NOMA system. Still, they have certain benefits, including higher signal quality and a better user experience. Also, fairness is constrained by things like how power is shared, who uses the channel, and how the channel is set up, which don't change much between different setups. The performance of the three systems is approximately equal to the SNR of -15 dB and then begins to diverge. At an SNR of 40 dB, the fairness index ratings for the three systems are 0.47, 0.658, and 0.48, respectively, with 100 users.

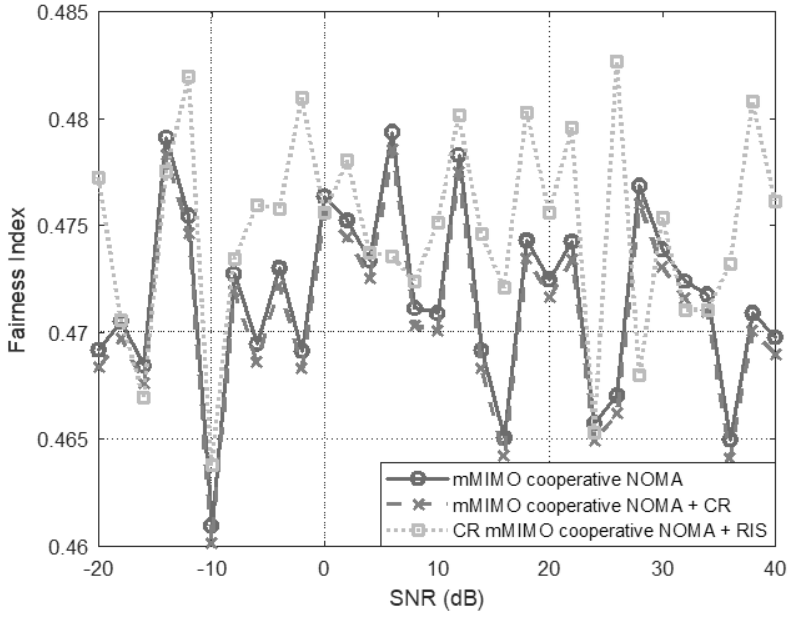

Fig. 11. Fairness index versus SNR for three different scenarios

Observe the variation of the fairness index as a function of SNR across three distinct systems in Figure 12: mMIMO cooperative NOMA, mMIMO CR cooperative NOMA, and mMIMO CR cooperative NOMA with intelligent RIS, and systems utilize the Q-learning approach. When the SNR is low, particularly at 5 dB, the system becomes unstable as it fails to provide equitable power distribution among users under adverse signal conditions, resulting in the loss of advantages from CR and RIS owing to significant interference. Additionally, Q-learning may struggle to balance exploration, seeking superior solutions, and exploitation by selecting the most effective known action, resulting in instability and suboptimal fairness.

With 100 users and 40 dB SNR, the fairness index performance levels for the three systems are 0.71851, 0.71214, and 0.72123, respectively. When comparing the performance of the fairness index ratio before and after using Q-learning, we find that the fairness index improvement rate for the three systems reached 20.9%, 20.4%, and 20%, respectively. Q-learning and RIS provide an effective approach to enhance fairness in cooperative NOMA systems by dynamically distributing power and optimizing signal conditions for weaker users, hence providing a more equitable performance across all users. These outcomes surpass those of [50-55].

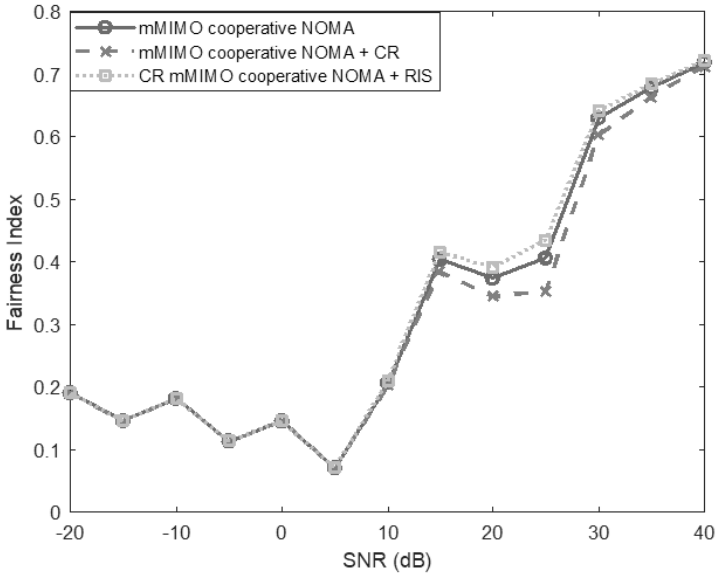

Fig. 12. Fairness index versus against SNR for three different scenarios with optimization technique

4. Conclusions

The proposed system achieves substantial enhancements in SE and throughput via the implementation of CR spectrum detection and intelligent phase shift optimization across diverse user configurations inside the mmWave environment. Studies show that adding RIS to CR-based mMIMO cooperative NOMA systems greatly lowers latency and packet loss while raising the fairness index, especially when there are a lot of users. The findings indicate that RIS-assisted cooperative NOMA is an optimal selection for future 6G networks, as it diminishes interference, enhances signal quality, and optimizes system performance under high mobility. The study's findings confirm the significant improvement and increasing importance of Q-learning approaches in reducing latency, packet loss, and the fairness index in high-

density mmWave environments. It adds a lot of benefits to the proposed system because it dynamically distributes power, which enables the system to adapt to user density and fluctuating network conditions, thus greatly reducing interference and resource competition. Future research will focus on significant improvements in system performance through better power allocation and user scheduling in RIS-enabled systems, in particular. The latency model is to be examined in some practical conditions, such as queuing delays, handover effects, and packet retransmissions.

References

[1]. W. Jiang, B. Han, M. A. Habibi, and H. D. Schotten, "The Road Towards 6G: A Comprehensive Survey," in IEEE Open Journal of the Communications Society, vol. 2, 2021, pp. 334-366.

[2]. F. Akyildiz, A. Kak, and S. Nie, "6G and Beyond: The Future of Wireless Communications Systems," in IEEE Access, vol. 8, pp.133995-134030, 2020.

[3]. F. Guo, F. R. Yu, H. Zhang, X. Li, H. Ji, and V. C. M. Leung, "Enabling Massive IoT Toward 6G: A Comprehensive Survey," in IEEE Internet of Things Journal, vol. 8, no. 15, pp. 11891-11915, 1 Aug. 2021.

[4]. M. Hassan, R. A. Saeed, R. A. Mokhtar, K. Hamid, E. S. Ali, N. Odeh, M. Singh, O. O. Khalifa, and S. Islam, "BER Improvement of Cooperative Spectrum Sharing of NOMA in 5G Network," in IEEE Access, vol. 3rd International Maghreb Meeting of the Conference on Sciences and Techniques of Automatic Control and Computer Engineering (MI-STA), pp. 647-652, 2023.

[5]. H. Ahmed, A. Thair Al-Heety, B. Al-Khateeb, and A. H. Mohammed, "Energy Efficiency in 5G Massive MIMO for Mobile Wireless Network," 2020 International Congress on Human-Computer Interaction, Optimization and Robotic Applications (HORA), Ankara, Turkey, pp. 1-6, 2020.

[6]. L. You, J. Xiong, A. Zappone, W. Wang, and X. Gao, "Spectral Efficiency and Energy Efficiency Tradeoff in Massive MIMO Downlink Transmission with Statistical CSIT," in IEEE Transactions on Signal Processing, vol. 68, pp. 2645-2659, 2020.

[7]. N. Amani, S. Parsaeefard, and H. Yanikomeroglu, "Multi-Objective Energy Efficient Resource Allocation in Massive Multiple Input Multiple Output-Aided Heterogeneous Cloud Radio Access Networks," in IEEE Access, vol. 11, pp. 33480-33497, 2023.

[8]. M. H. Babikir, K. Hamid, G. A. M. Abdu, I. Elsayed, R. A. Saeed and O. O. Khalifa, "Optimization Efficiency of 5G MIMO Cooperative Spectrum Sharing NOMA Networks," 2024 9th International Conference on Mechatronics Engineering (ICOM), Kuala Lumpur, Malaysia, pp. 183-187, 2024.

[9]. Y. Yuan, R. He, B. Ai, Z. Ma, Y. Miao, Y. Niu, J. Zhang, R. Chen, and Z. Zhong, "A 3D Geometry-Based THz Channel Model for 6G Ultra Massive MIMO Systems," IEEE Transactions on Vehicular Technology, vol. 71, no. 3, pp. 2251-2266, March 2022.

[10]. M. Hassan, R. A. Saeed, R. A. Mokhtar, K. Hamid, E. S. Ali, N. Odeh, M. Singh, O. O. Khalifa, and S. Islam, "NOMA Cooperative Spectrum Sharing Average Capacity Improvement in 5G Network," 2023 IEEE 3rd International Maghreb Meeting of the Conference on Sciences and Techniques of Automatic Control and Computer Engineering (MI-STA), Benghazi, Libya, pp. 653-658, 2023.

[11]. J. Wang, C. -X. Wang, J. Huang, H. Wang and X. Gao, "A General 3D Space-Time-Frequency Non-Stationary THz Channel Model for 6G Ultra-Massive MIMO Wireless Communication Systems," in IEEE Journal on Selected Areas in Communications, vol. 39, no. 6, pp. 1576-1589, June 2021.

[12]. M. Hassan, M. Singh and K. Hamid, "Survey on NOMA and Spectrum Sharing Techniques in 5G," 2021 IEEE International Conference on Smart Information Systems and Technologies (SIST), Nur-Sultan, Kazakhstan, pp. 1-4, 2021.

[13]. C. Wu, X. Mu, Y. Liu, X. Gu and X. Wang, "Resource Allocation in STAR-RIS-Aided Networks: OMA and NOMA," in IEEE Transactions on Wireless Communications, vol. 21, no. 9, pp. 7653-7667, Sept. 2022.

[14]. J. Chen and X. Yu, "Ergodic Rate Analysis and Phase Design of STAR-RIS Aided NOMA With Statistical CSI," in IEEE Communications Letters, vol. 26, no. 12, pp. 2889-2893, Dec. 2022.

[15]. H. Liu, G. Li, X. Li, Y. Liu, G. Huang and Z. Ding, "Effective Capacity Analysis of STAR-RIS-Assisted NOMA Networks," in IEEE Wireless Communications Letters, vol. 11, no. 9, pp. 1930-1934, Sept. 2022.

[16]. E., Basar, Di Renzo, M., De Rosny, J., Debbah, M., Alouini, M.-S., and Zhang, R. (2019). Wireless communications through reconfigurable intelligent surfaces. IEEE Access 7, 116753–116773..

[17]. Liu, Z., and Yang, L.-L. (2021). Sparse or dense: a comparative study of code-domain NOMA systems. IEEE Trans. Wirel. Commun. 20, 4768–4780, 2021.

[18]. Ohood Fadil Alwan (2023). Using Artificial Intelligence to Diagnose Demented in the Elderly, Al-Esraa University College Journal for Engineering, pp 107 – 140. V (5)-No. (8).

[19]. M. A. ElMossallamy, H. Zhang, L. Song, K. G. Seddik, Z. Han and G. Y. Li, "Reconfigurable Intelligent Surfaces for Wireless Communications: Principles, Challenges, and Opportunities," in IEEE Transactions on Cognitive Communications and Networking, vol. 6, no. 3, pp. 990-1002, Sept. 2020.

[20]. A. Araghi, M. R. Aref, M. R. A. Khandani, and M. R. A. K. M. Sadeghi, "Reconfigurable Intelligent Surface (RIS) in the Sub-6 GHz Band: Design, Implementation, and Real-World Demonstration," IEEE Access, vol. 10, pp. 2646-2655, 2022.

[21]. L. Dai, B. Wang, M. Wang, X. Yang, J. Tan, S. Bi, S. Xu, F. Yang, Z. Chen, M. Di Renzo, C. B. Chae, and L. Hanzo, "Reconfigurable Intelligent Surface-Based Wireless Communications: Antenna Design, Prototyping, and Experimental Results," IEEE Access, vol. 8, pp. 45913-45923, 2020.

[22]. S. Aboagye, A. R. Ndjiongue, T. M. N. Ngatched, O. A. Dobre and H. V. Poor, "RIS-Assisted Visible Light Communication Systems: A Tutorial," in IEEE Communications Surveys & Tutorials, vol. 25, no. 1, pp. 251-288, Firstquarter 2023.

[23]. B. Rana, S. S. Cho and I. -P. Hong, "Review Paper on Hardware of Reconfigurable Intelligent Surfaces," in IEEE Access, vol. 11, pp. 29614-29634, 2023.

[24]. Y. Mao, O. Dizdar, B. Clerckx, R. Schober, P. Popovski and H. V. Poor, "Rate-Splitting Multiple Access: Fundamentals, Survey, and Future Research Trends," in IEEE Communications Surveys & Tutorials, vol. 24, no. 4, pp. 2073-2126, Fourthquarter 2022.

[25]. H. Ge, N. Garg, A. Papaz and T. Ratnar, "A Rate-Splitting Approach for RIS-Aided Massive MIMO Networks with Transceiver Design," 2023 IEEE 24th International Workshop on Signal Processing Advances in Wireless Communications (SPAWC), Shanghai, China, pp. 541-545, 2023.

[26]. G. Zheng, M. Wen, Y. Chen, Y. -C. Wu and H. V. Poor, "Rate-Splitting Multiple Access in Wireless Backhaul HetNets: A Decentralized Spectral Efficient Approach," in IEEE Transactions on Wireless Communications, vol. 23, no. 3, pp. 2413-2427, March 2024.

[27]. G. Cao, M. Li, H. Yuan, W. Chen, L. Li and A. Raouf, "Error Performance of RIS-Assisted NOMA Networks with Imperfect Channel State Information," 2023 IEEE 97th Vehicular Technology Conference (VTC2023-Spring), Florence, Italy, pp. 1-5, 2023.

[28]. Q. Wu and R. Zhang, "Towards smart and reconfigurable environment: Intelligent reflecting surface aided wireless network", IEEE Commun. Mag, vol. 58, no. 1, pp. 106-112, Jan. 2020.

[29]. K. Liu, Z. Zhang, L. Dai, S. Xu and F. Yang, "Active reconfigurable intelligent surface: Fully-connected or sub-connected?", IEEE Commun. Lett., vol. 26, no. 1, pp. 167-171, Jan. 2022.

[30]. T. D. Perera, D. N. K. Jayakody, S. K. Sharma, S. Chatzinotas and J. Li, "Simultaneous wireless information and power transfer (SWIPT): Recent advances and future challenges", IEEE Commun. Surveys Tuts., vol. 20, no. 1, pp. 264-302, 1st Quart. 2018.

[31]. B. Zhao, C. Zhang, W. Yi and Y. Liu, "Ergodic Rate Analysis of STAR-RIS Aided NOMA Systems," in IEEE Communications Letters, vol. 26, no. 10, pp. 2297-2301, Oct. 2022.

[32]. R. H. Yoga Perdana, T. -V. Nguyen, Y. Pramitarini, K. Shim and B. An, "Deep Learning-based Spectral Efficiency Maximization in Massive MIMO-NOMA Systems with STAR-RIS," 2023 International Conference on Artificial Intelligence in Information and Communication (ICAIIC), Bali, Indonesia, pp. 644-649, 2023.

[33]. X. Liu, T. Wei, H. Liang, C. Guo and B. Liao, "Robust Beamforming for RIS-Assisted NOMA Systems with CSI Imperfection and Low-Resolution Phase Shifters," 2023 6th International Conference on Information Communication and Signal Processing (ICICSP), Xi'an, China, pp. 654-658, 2023.

[34]. J. Y. Baek, Y. -S. Lee and B. C. Jung, "Downlink RIS-NOMA with Constellation Adjustment for 6G Wireless Communication Systems," 2024 IEEE 21st Consumer Communications & Networking Conference (CCNC), Las Vegas, NV, USA, pp. 1076-1077, 2024.

[35]. J. Zhang, J. Zhang, Y. Zhou, H. Ji, J. Sun and N. Al-Dhahir, "Energy and Spectral Efficiency Tradeoff via Rate Splitting and Common Beamforming Coordination in Multicell Networks," in IEEE Transactions on Communications, vol. 68, no. 12, pp. 7719-7731, Dec. 2020.

[36]. S. Ghosh, A. Bhowmick, S. D. Roy and S. Kundu, "Outage and Ergodic Capacity Analysis in UAV-RIS Assisted NOMA-D2D Network," 2023 IEEE International Conference on Advanced Networks and Telecommunications Systems (ANTS), Jaipur, India, pp. 762-767, 2023.

[37]. Z. Zhu and X. Huang, "Connectivity of Wireless Networks Assisted by Transmissive Reconfigurable Intelligent Surfaces," 2023 IEEE 98th Vehicular Technology Conference (VTC2023-Fall), Hong Kong, Hong Kong, pp. 1-6, 2023.

[38]. P. Tulupov, B. Sorokin and A. Korolev, "Coverage impact of reconfigurable intelligent surfaces in 6G mobile networks," 2022 International Conference on Electrical, Computer and Energy Technologies (ICECET), Prague, Czech Republic, pp. 1-5, 2022.

[39]. M. Tavana, M. Masoudi and E. Björnson, "Dynamic RF Charging of Zero-Energy Devices via Reconfigurable Intelligent Surfaces," in IEEE Wireless Communications Letters, vol. 13, no. 8, pp. 2295-2299, Aug. 2024.

[40]. A. U. Makarfi, R. Kharel, K. M. Rabie, O. Kaiwartya, X. Li and D. -T. Do, "Reconfigurable Intelligent Surfaces based Cognitive Radio Networks," 2021 IEEE Wireless Communications and Networking Conference Workshops (WCNCW), Nanjing, China, pp. 1-6, 2021.

[41]. A. El Mettiti, M. Saber, A. Chehri, H. Chaibi, A. Badaoui and R. Saadane, "Reconfigurable Intelligent Surfaces and DF-relay Improved Spectral Efficiency in Cognitive Radio Networks," 2023 IEEE 97th Vehicular Technology Conference (VTC2023-Spring), Florence, Italy, pp. 1-6, 2023.

[42]. Y. Youn, D. An, D. Kim, M. Hwang and W. Hong, "Cognitive Reconfigurable Intelligent Surface (RIS) for mmWave Integrated Sensing and Communication," 2023 IEEE International Symposium on Antennas and Propagation (ISAP), Kuala Lumpur, Malaysia, pp. 1-2, 2023.

[43]. M. O. Hasna, "Optimization of Effective Area Spectral Efficiency for Wireless Communications Systems under Nakagami-m Fading Channels," 2016 IEEE 84th Vehicular Technology Conference (VTC-Fall), Montreal, QC, Canada, pp. 1-6, 2016.

[44]. J. Li, Z. Song, T. Hou, J. Gao, A. Li and Z. Tang, "An RIS-Aided Interference Mitigation-Based Design for MIMO-NOMA in Cellular Networks," in IEEE Transactions on Green Communications and Networking, vol. 8, no. 1, pp. 317-329, March 2024.

[45]. E. Basar, G. C. Alexandropoulos, Y. Liu, Q. Wu, S. Jin, C. Yuen, O. A. Dobre, and R. Schober, "Reconfigurable Intelligent Surfaces for 6G: Emerging Hardware Architectures, Applications, and Open Challenges," IEEE Vehicular Technology Magazine, vol. 19, no. 3, pp. 27-47, Sept. 2024.

[46]. A. A. Yassin, M. A. Al-Husseini, and M. A. Al-Qutayri, "Reconfigurable Dual Band Antenna for 2.4 and 3.5 GHz Using Single PIN Diode," in 2013 International Conference on Computing, Electrical and Electronics Engineering (ICCEEE), pp. 63-66, 2013.

[47]. Gevez Yarkin, Tek Yusuf Islam, and Basar Ertugrul, Dynamic RIS partitioning in NOMA systems using deep reinforcement learning, Frontiers in Antennas and Propagation, Vol. 2, 2024.

[48]. X. Mu, Y. Liu, L. Guo, J. Lin and N. Al-Dhahir, "Capacity and Optimal Resource Allocation for IRS-Assisted Multi-User Communication Systems," in IEEE Transactions on Communications, vol. 69, no. 6, pp. 3771-3786, June 2021.

[49]. H. Zhou, M. Erol-Kantarci, Y. Liu and H. V. Poor, "A Survey on Model-Based, Heuristic, and Machine Learning Optimization Approaches in RIS-Aided Wireless Networks," in IEEE Communications Surveys & Tutorials, vol. 26, no. 2, pp. 781-823, Second quarter 2024.

[50]. G. C. Alexandropoulos *et al.*, "RIS-enabled smart wireless environments: Deployment scenarios network architecture bandwidth and area of influence", EURASIP J. Wireless Commun. Netw., vol. 103, pp. 1-38, Oct. 2023.

[51]. B. B. Murti, R. Hidayat and S. B. Wibowo. Spectrum Sensing Using Adaptive Threshold Based Energy Detection in Cognitive Radio System. 2021 4th International Seminar on Research of Information Technology and Intelligent Systems (ISRITI), Yogyakarta, Indonesia, pp. 614-617, 2021.

[52]. Vu, T.-H. *et al.* "RIS-Aided Cognitive NOMA Networks: Deep Learning Evaluation." IEEE Trans. Wireless Commun., 21(12), 10662–10677, 2022.

[53]. De Sena, A.S. *et al.* "Massive MIMO-NOMA Networks With Imperfect SIC: Design and Fairness Enhancement." IEEE Trans. Wireless Commun., 19(9), 6100–6115, 2020.

[54]. Solaiman, S. *et al.* "User Clustering and Optimized Power Allocation for D2D Communications at mmWave Underlaying MIMO-NOMA Networks." IEEE Access, 9, 57726–57742, 2021.

[55]. F. Kara and H. Kaya, "Improved User Fairness in Decode-Forward Relaying Non-Orthogonal Multiple Access Schemes With Imperfect SIC and CSI," in IEEE Access, vol. 8, pp. 97540-97556, 2020.